表1　血栓止血関連検査

A 血小板系検査
- 血小板数
- 出血時間
- 血小板機能検査
  - 血小板凝集能
  - (Born の比濁法，散乱光粒子計測法など)
  - 血小板停滞率
  - (ガラスビーズカラム法，プラビーズカラム法など)
  - 血小板放出能 (セロトニン放出アッセイなど)
  - 血餅収縮能
- 血小板活性化マーカー
  - 血小板第4因子 (PF4)
  - β-トロンボグロブリン
  - VASP リン酸化
  - 血小板マイクロパーティクル
  - 血小板表面マーカー
- 血小板寿命
- 血小板機能簡易検査
  - (PFA-100，VerifyNow，Plateletworks など)

B 凝固系検査、抗凝固系検査
- プロトロンビン時間 (PT)
- 活性化部分トロンボプラスチン時間 (APTT)
- 活性化凝固時間 (ACT)
- フィブリノゲン量
- 凝固因子活性測定
- トロンボテスト
- ヘパプラスチンテスト
- 循環抗凝血素
- ループスアンチコアグラント
- トロンビン－アンチトロンビン複合体 (TAT)
- プロトロンビンフラグメント F_{1+2} (F_{1+2})
- 凝固簡易検査 (CoaguCheck など)
- アンチトロンビン
- プロテイン C
- プロテイン S

C 線溶検査
- プラスミノゲン
- フィブリン・フィブリノゲン分解産物 (FDP)
- D-ダイマー
- プラスミン・α_2 プラスミンインヒビター複合体 (PIC)
- 組織プラスミノゲンアクチベータ
- プラスミノゲンアクチベータインヒビター-1 (PAI-1)

D フォンウィルブランド因子検査
- フォンウィルブランド因子抗原
- フォンウィルブランド因子活性

E 包括的検査 (血管・血液・血流)
- 毛細血管抵抗試験 (生体検査)
- 凝固波形解析
- ROTEM アッセイ
- トロンビン生成能
- T-TAS

G 血栓症自己免疫検査
- 抗リン脂質抗体
- HIT 抗体
- ADAMTS13 インヒビター

そして治療によって起こる出血，血栓など有害事象の予測にも用いられる．

1) 出血傾向に関する検査

出血傾向の診断には通常，問診，身体所見，スクリーニング検査，そして確定のための二次検査が行われる (図1)[1]．

①問診，身体所見

病歴：出血傾向の診断には問診が非常に重要である．既往症 (過去の抜歯，手術) や，家族歴，服薬歴，出血の誘因 (感染の有無など) のほか随伴症状 (発熱，腹痛，関節痛，レイノー症状) を聴取する．

身体所見：出血斑の分類 (petechia，echymosis)，出血斑の性状 ("palpable" または "non palpable" 熱感，圧痛，かゆみの有無)，関節の腫脹の有無，リンパ節腫脹の有無，肝脾腫の有無，などに注意する．

近年，出血症状をより客観的に評価するため，症状をスコア化する方法が国際血栓止血学会 (International Society of Thrombosis and Hemostasis : ISTH) より報告されている．出血症状を出血部位ごとにそれぞれ5段階評価し，総合して判断するもので，スコアが高いほど出血症状が強いと判断される[2]．

②スクリーニング検査

病歴聴取や身体所見を基にまず血小板の異常について血小板数を，凝固異常について APTT (活性化部分トロンボプラスチン時間)，PT (プロトロンビン時間)，フィブリノゲン，その他 (肝機能，腎機能，蛋白分画，免疫グロブリン) を測定する．これらスクリーニング検査により出血性疾患を大まかに分類し (図2)[1]，さらに2次検査により疾患を特定する．出血時間は侵襲的検査であるので，血小板数が正常以上で一次止血の異常が疑われる場合に行う．スクリーニングがすべて正常で明ら

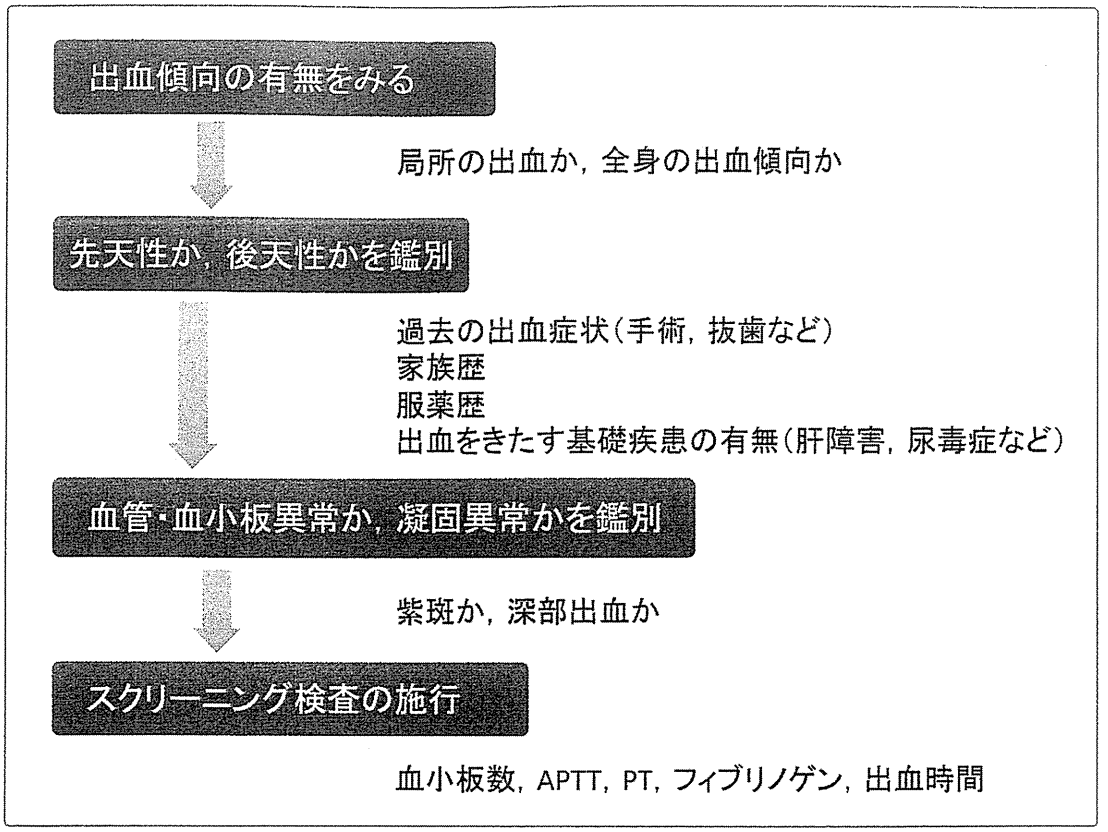

図1　出血傾向診断手順の概略（文献1より引用改変）

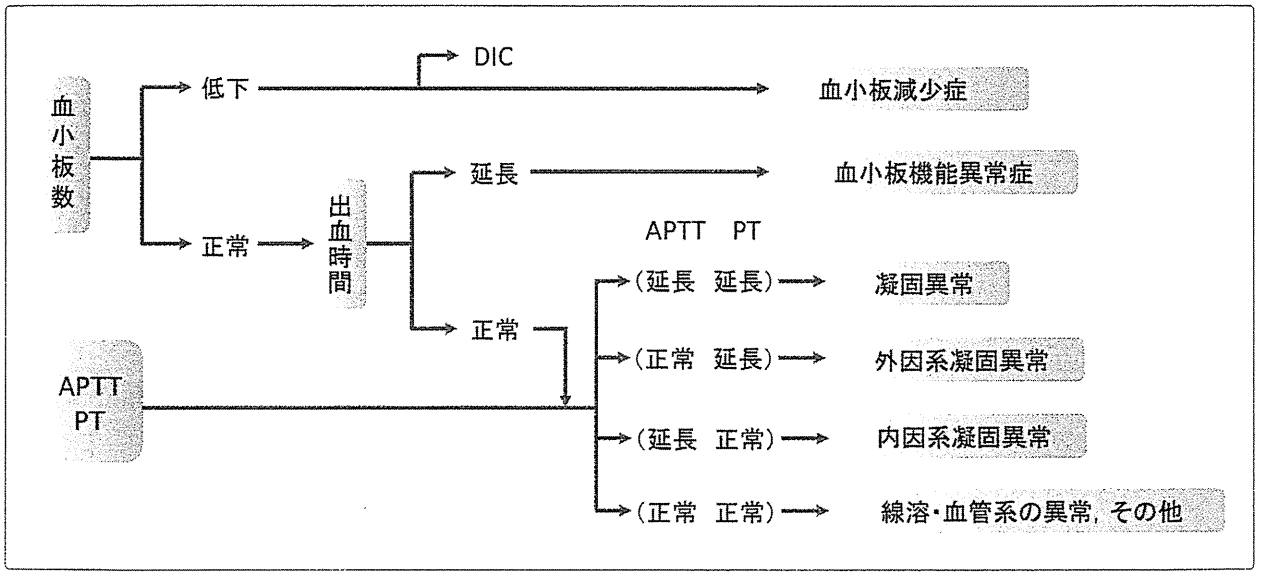

図2　スクリーニング検査による出血傾向の原因分類（文献1より引用改変）

かに出血傾向を認めれば，血管異常や線溶亢進（FDP，PIC，プラスミノゲン，α_2-プラスミンインヒビター（α_2-PI）などを参考にする）や凝固第XIII/13因子欠乏症（FXIII/13が正常の1%以下）を疑う．

③ Second line 検査

スクリーニング検査の結果に基づき特定の検査を行い診断を確定する．詳細は各項に譲る．

2）血栓症，血栓性素因に関する検査

血栓症（血栓傾向）に関する検査には画像検査，生体機能検査，検体検査が含まれるが，ここでは検体検査について述べる．血栓の存在そのものを同定する検査と，血栓傾向を予測する検査がある．

前者はFDPやDダイマー，トロンビンーアンチトロンビン複合体（TAT）に代表され，後者はアンチトロンビン（AT），プロテインC（PC），プロテインS（PS），抗リン脂質抗体などが代表的である．

血栓傾向（易血栓性）に共通の検査所見として凝固能の亢進（APTTの短縮やFDPやDダイマーの軽度上昇，プロトロンビンフラグメントF_{1+2}(F_{1+2})の増加），血小板機能の亢進（凝集能の亢進）などが認められることがあるが，なくても血栓傾向は否定できない．先天性血栓性素因を疑った場合，通常まずAT，PC，PS，プラスミノゲン，フィブリノゲンなどの活性を測定する．診断がつかなければさらにヘパリンコファクターII，α_2-PI，プラスミノゲンアクチベーターインヒビター-1（PAI-1）などを測定するが，これらの異常が原因となることは稀である．血栓の存在を示すいわゆる凝固系の診断マーカーとして，TATとF_{1+2}は，トロンビン生成の指標と考えられているが，特異性に問題があり注意を要する．このほかフィブリン生成の指標としては可溶性フィブリンモノマーなどがある．一方，線溶マーカーとしてはフィブリン分解産物（FDP，D-ダイマー）のほかプラスミンープラスミンインヒビター複合体（PIC）が一般的である．

4　血栓止血関連検査の最近の動向

過去には出血傾向をいかに鋭敏かつ特異的に捉えるか，すなわち出血傾向を捉える研究に主眼が置かれていたが，近年わが国でも血栓症が増加し，抗血栓薬使用の増加，そして新しい抗血小板薬や抗凝固薬の登場と相まって，血栓傾向の診断や抗血栓薬のモニタリングの重要性が高まっている．

たとえば抗血小板薬の効果の評価にはいくつか血小板機能検査が使用されている．近年，全血で短時間に検査可能な機器が多く開発されており，これらを用いた臨床研究も数多くみられ，モニタリングの有用性を示す論文も多い．しかしながら個々の臨床研究で用いられる検査機器が異なっている，また同じ検査機器を用いて標準化が遅れており，たとえばカットオフ値も研究ごとにまちまちである，など問題点も多い．各論は以下の章に譲るが，今後は個々の薬剤に対してきめ細かな検査法の確立が臨床検査に求められているといえよう．さらに最近主流の抗血小板薬は分子標的が明確になっているため，本来は標的分子の評価をすべきことは明白である．

一方，抗凝固薬に目を向ければ深部静脈血栓症，肺血栓塞栓症は人口の高齢化で増加し，また術後血栓症として安全対策の観点から近年注目度が高い．治療の進歩は最近まで緩やかであったが，ここ数年で大きな変革が起きている．すなわち，半世紀以上も治療のトップに君臨してきたワルファリンやヘパリンが新薬にとってかわられようとしている．新薬は作用点が特異的であり，モニター検査はその標的分子にターゲットを当てるべきである．さらに薬物によっては従来型の凝固能（APTTやPT）に反映されないものも登場しており，まさに治療の進歩に検査が追いついていない状況が発生している．新たな検査の開発，普及が求められている．

おわりに

止血障害，血栓性疾患はどの診療科でも遭遇する頻度の高い病態であり，特に血栓症は21世紀の国民病ともいわれその治療や予防に用いられる薬物（止血薬，抗血小板薬や抗凝固薬などの抗血栓薬，血液製剤，生物製剤など）には莫大な医療費が投じられている．それぞれの疾患，そして個々の病態により治療の効果には個体差が大きく，安全，効率的な治療にはモニター検査が重要である．しかるにこれまで長期に渡り実用に供されていた血小板／凝固線溶検査については一部自動化されているものの，手技の複雑さや影響を受ける因子の多さなどから理想的なモニター検査とは程遠い．またAPTTやPTは凝固能をoverallで捉える一種の機能検査であり，本来の薬剤標的を特異的に捉えているものではない．血小板機能検査は一部の簡易迅速検査が脚光を浴びているが，従来型は煩雑で標準化にはまだまだ険しい道のりが

ある．今後は新薬として分子標的が明確な抗血小板薬や抗凝固薬が主流になると思われ，それぞれの薬剤に対応した精度の高いモニター検査が求められる．新しい臨床検査が確立されるまでには多くの道のりがある．一次研究で候補の検査が発見されてもすぐに臨床応用できるわけではない．論文の系統的レビュー，検査方法論の確立，臨床での意志決定（decision making）における有用性，安全性，倫理性の評価，経済性の評価などがクリアされ，保険医療への適応を経て成熟した臨床検査となる．さらに検査の標準化，電子データの医療機関内や医療機関間の共有システムなどがその後の課題となる．少子高齢化社会の中，医療スタッフは限られた資源で知恵を絞り，効率的な医療を行わねばならない．止血異常や血栓性素因の評価，治療による患者の変化を鋭敏に捉える検査が必要であり，臨床検査のさらなる発展が求められる．止血／血栓関連検査の標準化を進めること，新たな治療に対して検査が遅れをとらずに研究開発されることが肝要であるが，加えて従来型の血小板機能検査や凝固検査から脱却し，それぞれの血栓症治療薬に特異的な新しい臨床検査指標を包括的に探索開発することも必要である．臨床検査の発展により，止血異常／血栓症の治療が今以上に効果的かつ安全に行われるものと考える．

参考文献

1) 村田　満．出血性疾患の診断アプローチ．In: 柴田　昭，他編．エッセンシャル血液病学．第5版．東京：医歯薬出版，2005; 221-226.
2) Rodeghiero F, Tosetto A, Abshire T, et al. ISTH/SSC joint VWF and Perinatal/Pediatric Hemostasis Subcommittees Working Group. ISTH/SSC bleeding assessment tool: a standardized questionnaire and a proposal for a new bleeding score for inherited bleeding disorders. J Thromb Haemost 2010; 8(9): 2063-2065.

止血・血栓

ハンドブック

編集
鈴木重統
後藤信哉
松野一彦

西村書店

7 血小板と止血

はじめに

血小板は生体内での止血機能調節において重要な役割を演じている細胞である。平常状態では，血液は生体内では凝固しない。しかし出血の際に血管から血液が流れ出すと，その血管傷害部位に血小板が集まり(一次止血)，さらに血液凝固因子によるフィブリン網が形成され強固な血液凝固塊の形成に至る(二次止血)(図1)[1]。血液凝固塊による止血が不要になる際には，線溶因子の働きにより血液凝固塊は少しずつ溶解される。

本稿では，止血機構における血小板の役割，そして血小板の量的・質的異常による出血傾向に関して概説したい。

止血機構における血小板の役割(一次止血)

血小板は刺激により粘着など血小板内顆粒の放出を伴わない可逆的な一次凝集と，顆粒放出を伴い強固な血小板凝集塊を呈する二次凝集がある。血管が傷つき露呈した血管内皮下組織のコラーゲン，あるいはコラーゲンに粘着したvon Willebrand(フォン・ヴィルブランド)因子(VWF)と血小板膜受容体が可逆的に反応する。

これらの反応により血小板活性化シグナルが血小板の細胞内に伝達され，血小板は偽足を出す形態変化を伴いながら，血小板内顆粒物質を放出する。それら物質は，さらに血小板活性化に作用する。顆粒は，アデノシン二リン酸(adenosine diphosphate：ADP)，アデノシン三リン酸(adenosine triphosphate：ATP)，セロトニン，フィブリノゲン，VWF，血小板第4因子(platelet factor 4：PF4)，血小板由来増殖因子(platelet-derived growth factor：PDGF)，フィブロネクチン，第Ⅴ因子，β-トロンボグロブリン，P-セレクチン，トロンボスポンジンを含む。同様に活性化血小板から放出されるトロンボキサンA_2も血小板膜に存在する受容体を介して強力な血小板活性化作用を示す。

表1に示すように，血小板活性化に関与する膜受容体は数多く，さらにそれぞれが異なる経路を用いて血小板活性化を調節している。たとえば，GP(糖蛋白(glycoprotein))Ⅰb/Ⅸ/ⅤとVWFの反応は一次凝集において主たる働きを示し，ADPとP2Y1は一次凝集，ADPとP2Y12は二次凝集に関与する。

表1 主な血小板膜受容体とリガンド

血小板膜受容体	リガンド
GPⅠa/Ⅱa	コラーゲン
GPⅠb/Ⅸ/Ⅴ	von Willebrand因子
GPⅡb/Ⅲa	フィブリノゲン，von Willebrand因子
GPⅥ	コラーゲン
GPⅥ	コラーゲン
α_2アドレナリン受容体	エピネフリン
P2Y1	ADP
P2Y12	ADP
プロテアーゼ活性化受容体(PAR)	トロンビン
セロトニン受容体	セロトニン
トロンボキサンA_2受容体	トロンボキサンA_2

GP：糖蛋白，ADP：アデノシン二リン酸

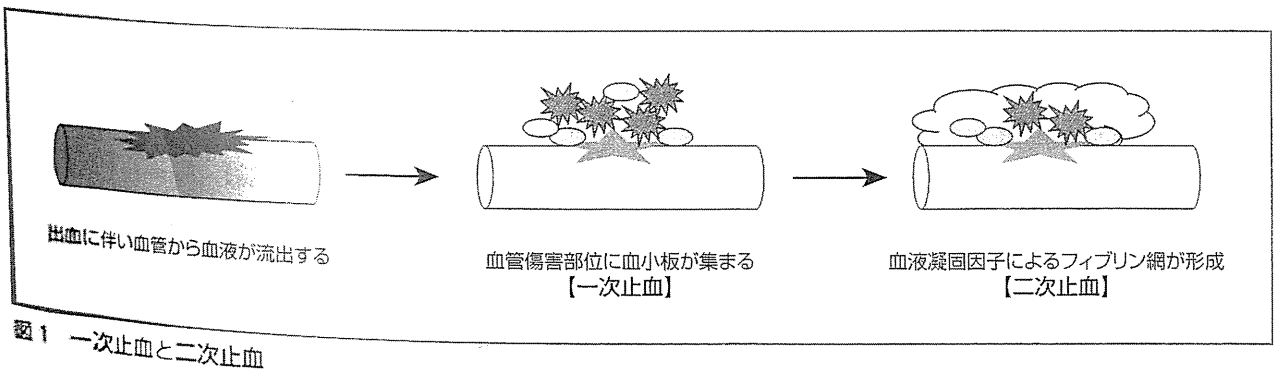

図1 一次止血と二次止血

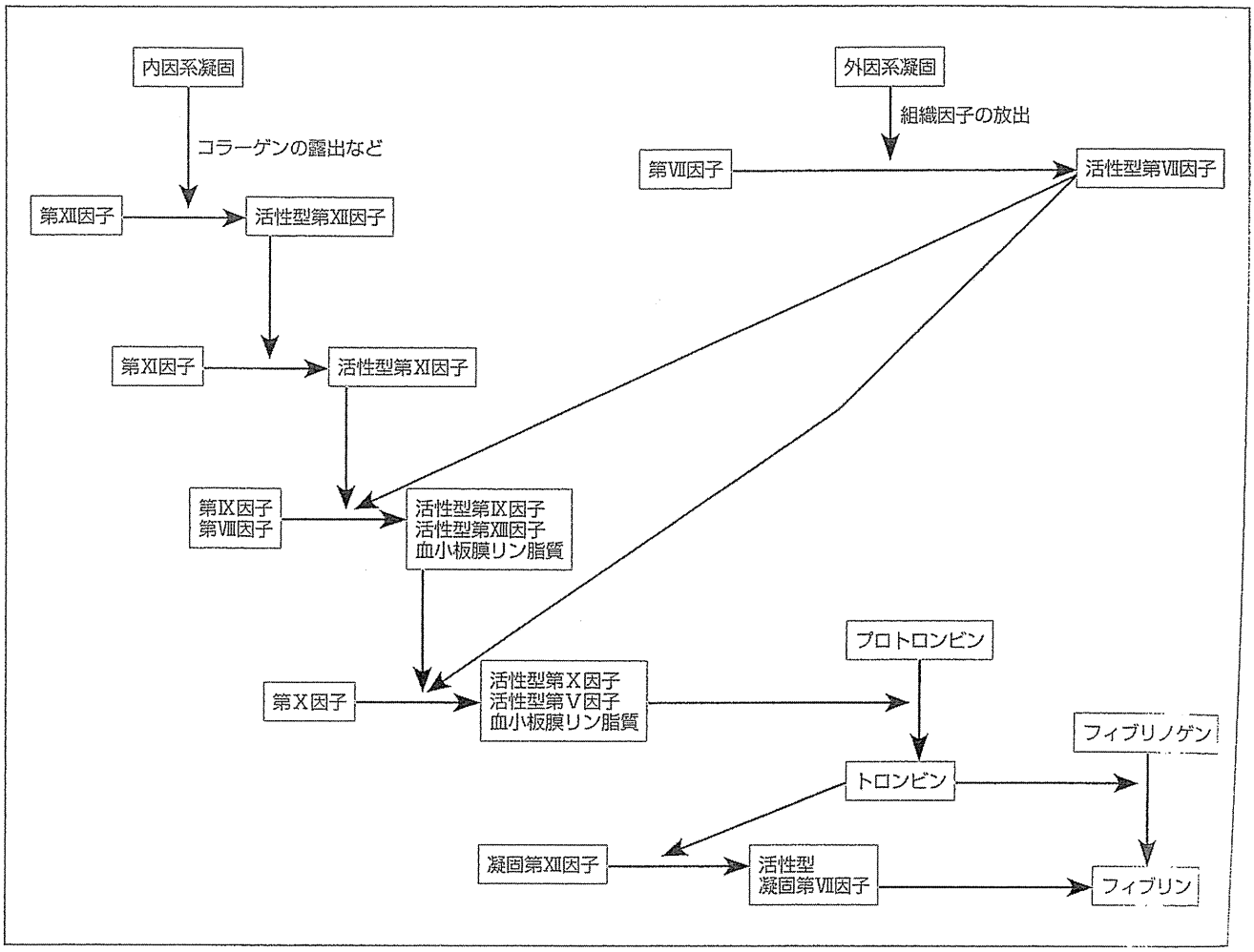

図2　血液凝固カスケード

このように血小板は，多様な機序により止血機能を調節している[2),3)]。したがって，これら血小板膜受容体やリガンドのいずれかに量的・質的な異常が生じた場合は，症状の程度に幅はあるが，出血傾向につながっていく（血小板の量的・質的な異常による出血傾向に関しては後述）。

止血機構における二次止血

図1に示すように，血小板が主体となる一次止血に引き続き，さらに血液凝固因子によるフィブリン網が形成され，強固な血液凝固塊の形成に至る。血液凝固反応は内因系凝固，外因系凝固，線溶系，そして凝固阻止系の因子が制御している。血管内皮細胞が傷害を受けることにより，血液凝固因子が主体となる凝固系反応の亢進が起こる（図2，図3）。

血管障害部位に露呈された陰性荷電物質が第XII因子の陽性荷電領域に結合し，活性型第XII因子（F

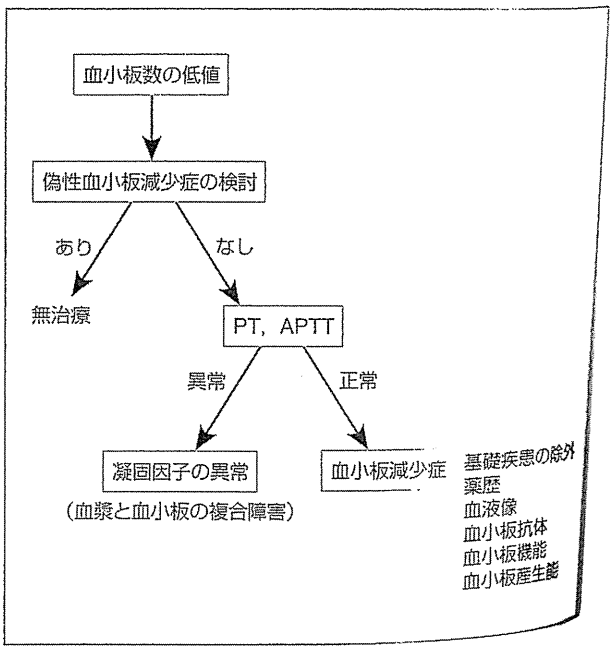

図3　血小板減少症の鑑別診断
PT：プロトロンビン時間，APTT：活性化部分トロンボプラスチン時間

XIIa)となることが内因系凝固反応スタートの主な機序である。FXIIaは第VII因子を活性化して外因系凝固に働きかける。またFXIIaは第XI因子も活性化させる。外因系凝固反応は血管障害を受け，露呈した血管内皮下組織に多量に存在する組織因子(tissue factor：TF)に対する第VII因子の結合からスタートする。この後，内因系凝固と外因系凝固の共通の凝固反応経路である第X因子の活性化，プロトロンビンの活性化によってトロンビンが生成される。

凝固反応の最終段階の主要な反応は，トロンビンによるフィブリノゲンからフィブリンへの反応である。血液凝固阻止反応として，アンチトロンビン(antithrombin：AT)はヘパリンを補因子として，トロンビン，活性型第X因子(FXa)，あるいは活性型第XI因子(FXIa)の作用を阻害する。

血小板と凝固因子の反応に関しては，内因系凝固におけるFXIaと血小板膜リン脂質との結合による第X因子の活性化作用に関与し，FXaはプロトロンビンをトロンビンにする。トロンビン受容体は血小板膜に存在しており，これら反応を介してさらに強固な凝集塊が形成される。

このように，活性化血小板による血小板凝集塊は，血液凝固因子の反応の促進の場となり，血小板と血液凝固因子の相互作用により最終的に血液凝固塊が形成される

血小板の量的・質的異常による出血傾向

出血傾向は血小板の異常や凝固・線溶因子の異常により起こる。本稿では血小板に焦点をあて述べていきたい。血小板の量的・質的異常による出血傾向に関与する因子は多様であり，また先天性と後天性のものがある。

血小板に起因する出血傾向は，血小板減少や血小板機能異常が主な原因である。血小板減少は，血小板の産生低下あるいは血小板の破壊亢進や消費，脾腫による体内分布の異常によるものがあり，その重症度は，軽度(50,000～150,000/μL)，中程度(20,000～50,000/μL)，重度(<20,000/μL)に分類されるが，疾患により精査や治療の必要性に幅があることに注意したい。また，先天性血小板減少症も報告されている。血小板減少による出血傾向は紫斑(点状出血や斑状出血)や粘膜出血，月経過多が認められる。

検査の手順は，自動血球計数装置により血小板数の低値を認めた場合は，末梢血塗抹標本を観察して，偽性血小板減少症や巨大血小板の有無を判別する(図3)。偽性血小板減少症は，自動血球計数装置を用いている場合に0.1～1%の頻度で認められる。偽性血小板減少症では，採血管内で抗凝固薬EDTA(エチレンジアミン四酢酸)の存在下，免疫グロブリンにより血小板どうしあるいは血小板と白血球が結合することによる機序，あるいは血小板の荷電など血小板そのものに起因する機序により血小板凝集塊が生じ，自動血球計数装置では血小板と認識されず，血小板数が実際より少なくカウントされる。

機序に関しては不明点が多い。EDTA加血の末梢血塗抹標本では，血小板の凝集塊が認められるため判別できる。また，抗凝固薬としてEDTAではなく，クエン酸やヘパリンを用いた血小板数測定でも偽性血小板減少症を判別できる。

EDTA偽性血小板減少症は，疾患特異性はないとされている。末梢血塗抹標本の観察により偽性血小板減少症の除外や形態観察を行い，巨大血小板の有無など確認後，プロトロンビン時間(prothrombin time：PT)や活性化部分トロンボプラスチン時間(activated partial thromboplastin time：APTT)を測定する。これらの検査により凝固・線溶系の異常を検討する。次いで鑑別診断(基礎疾患の除外，薬歴，血小板抗体，血小板機能，血小板産生能)を進める。

血小板機能検査は，アゴニスト惹起血小板凝集能検査を行う。アゴニストとして，コラーゲン，ADP，エピネフリン，リストセチンが用いられる。また，刺激による血小板活性化の検討を行うためにCD62P(P-セレクチン)表面発現解析が行われることもある[4]。血小板減少症においてすべての症例に治療が行われることはない。出血傾向や血小板減少が重篤な場合は，ステロイドやγグロブリン療法，血小板輸血が行われる。

生体内において，血小板は骨髄において造血幹細胞から巨核球分化を経て，成熟巨核球より放出される[5]。骨髄における血小板産生低下は再生不

良性貧血，異形成症候群(myelodysplastic syndrome：MDS)，発作性夜間ヘモグロビン尿症，造血器腫瘍，骨髄線維症，固形癌の骨髄転移，化学療法後に認められる。後述する血小板破壊や消費亢進による特発性血小板減少性紫斑病(idiopathic thrombocytopenic purpura：ITP)のなかでも巨核球形成機能低下や血小板放出異常を示唆するものが存在するという報告もある。

感染症に合併する血小板減少も知られている。EB(Epstein-Barr)ウイルス，サイトメガロウイルス，ヒト免疫不全ウイルス(human immunodeficiency virus：HIV)，ヘルペスウィルス感染症，流行性耳下腺炎，麻疹，風疹，水痘，ウイルス出血熱，などで血小板減少が認められる。特にウイルス性出血熱に伴う血栓性血小板減少性紫斑病(thrombotic thrombocytopenic purpura：TTP)は著しい出血症状を呈する。また，細菌では*H. pylori*(ヘリコバクター・ピロリ〈*Helicobacter pylori*〉)感染症や結核，大腸菌O157感染症でしばしば合併する溶血性尿毒症症候群(hemolytic-uremic syndrome：HUS)で血小板減少が認められる。

血小板上には，ヒト血小板特異抗原(human platelet-specific antigen：HPA)，ヒト白血球抗原(human leukocyte antigen：HLA)などの同種抗原が存在する。繰り返しの血小板輸血や妊娠によって産生される血小板に対する同種抗体は血小板を破壊し，血小板減少をきたす。新生児同種免疫性血小板減少症(neonatal alloimmune thrombocytopenia：NAIT)，輸血後紫斑病(post transfusion purpura：PTP)，輸血による受動免疫性血小板減少症では，抗血小板同種抗体による血小板減少を呈する。血小板減少は出血によるものだけではなく，血栓症によっても引き起こされる。播種性血管内凝固症候群(disseminated intravascular coagulation：DIC)，TTP，抗リン脂質抗体症候群(antiphospholipid syndrome：APS)，ヘパリン起因性血小板減少症(heparin-induced thrombocytopenia：HIT)と多様であるが，これら疾患に対しては血小板減少症の配慮が必要である。

TTPは；血小板減少，溶血性貧血，腎機能障害，精神神経障害，発熱の5徴候が広く知られているが，近年の概念では，他の疾患の除外と血小板減少，溶血性貧血がTTP診断に必須とされるようになってきた。末梢血塗抹標本で破砕赤血球が観察されると，TTPの可能性が高くなる。TTPの原因とされるVWFの切断酵素ADAMTS13(a disintegrin-like and metalloproteinase with thrombospondin type1 motifs 13)活性低下を確認することが確定診断には重要である。TTPは2つに大別され，1つはADAMTS13遺伝子異常による先天性TTPあるいはUpshow-Schulman(アップショウ-シュールマン)症候群と呼ばれている。もう1つは後天性TTPであり，その多くの原因はADAMTS13に対する自己抗体出現と考えられている。

TTPと鑑別困難な疾患として血小板減少，溶血性貧血，腎不全の3徴候で知られるHUSがある。TTPとHUSは両疾患の病態名を含む血栓性微小血管障害症(thrombotic microangiopathy：TMA)が診断名として用いられることがある[6]。TMAは，頻度は低いが薬物(チエノピリジン誘導体，マイトマイシンC，PEG-インターフェロン〈PEG-IFN〉，バイアグラ)によって引き起こされるという報告がある。全身性エリテマトーデス(systemic lupus erythematosus：SLE)，慢性肝疾患，妊娠時に相対的に頻度高く認められる。TMAの治療には，血漿交換療法，FFP(新鮮凍結血漿〈fresh frozen plasma〉)輸注，ステロイド，ステロイドのパルス療法，抗血小板薬，透析，抗凝固薬，などがある。濃厚血小板輸血の単独投与はTMAの予後を悪化させると知られている。

血小板破壊や消費亢進による血小板減少としては，ITPがよく知られている。ITPは，抗血小板抗体により血小板破壊が亢進し，血小板減少をきたす自己免疫疾患である。近年，国際的には「免疫性血小板減少性紫斑病」と名称が変更されているが，日本では「特発性血小板減少性紫斑病」の名称が用いられている。抗血小板抗体は，GPⅡb/Ⅲaやグリコプロテイン(GP)Ⅰbaなど血小板膜糖蛋白受容体を主な標的とする。抗血小板抗体は血小板表面に結合し，自己抗体が結合した血小板はFcγ受容体や補体受容体を介してマクロファージなどに捕捉され

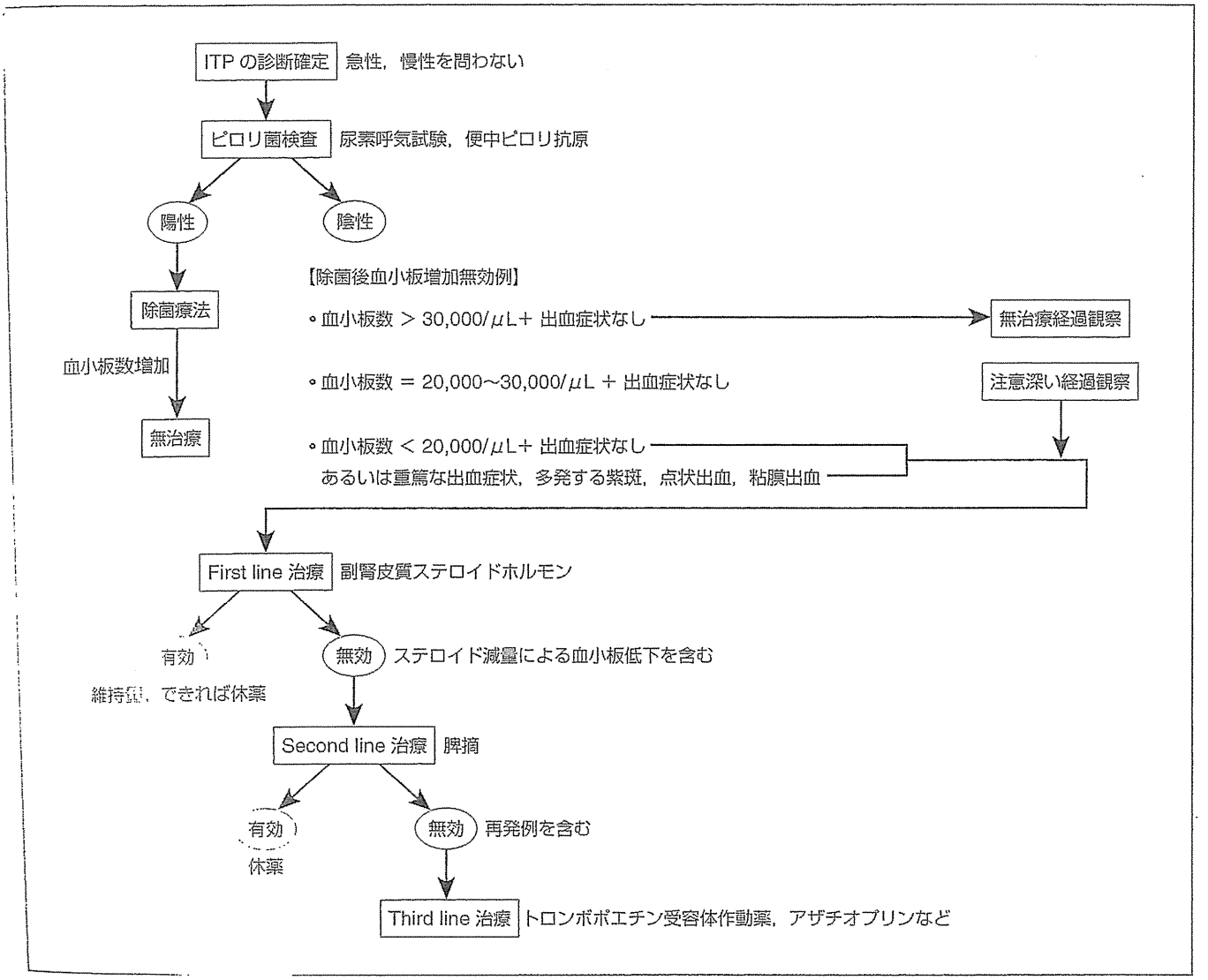

図4 成人ITP治療[7]
ITP：特発性血小板減少性紫斑病

食・破壊される．血小板膜糖蛋白受容体は巨核球にも発現していることから，抗血小板抗体は巨核球にも結合する．

ITPの診断基準は，後天性の血小板減少症（血小板数100,000/μL以下），臨床症状として皮膚の紫斑，粘膜出血など種々の出血症状を繰り返す，赤血球系，白血球系に量的・質的異常を認めない，ことである。他に特殊検査として，網血小板の増加や血漿トロンボポエチンの軽度の上昇，抗GP IIb/IIIa抗体や血小板抗体産生B細胞の末梢血中増加に加え，除外診断として血小板減少をきたす基礎疾患や原因が認められないことである。治療に関しては，2012年に成人ITP治療の参照ガイドが発表された（図4）[7]．

血小板の産生機構は多くの因子が複雑に制御していると考えられているが，遺伝子の関与も報告されている。そのなかでも遺伝的な要因には，血小板産生異常や機能異常を呈する先天性疾患の原因となる遺伝子変異が報告されている。先天性血小板機能異常に関する診断フローチャートについて，2012年に行われた国際血栓止血学会標準化委員会の血小板部会において提示された案を図5に示す。

血小板の膜受容体の1つであるGPIb/IX/V複合体のサブユニットGPIbα，GPIbβ，GPIXの遺伝子変異は，Bernald-Soulier（ベルナール-スリエ）症候群（BSS）の原因となる。GPVの遺伝子変異は報告されていない。BSS患者血小板では，対応する遺伝子産物の発現量減少や欠損を呈し，巨大血小板を示す。しかしすべての血小板が巨大ではなく，標本上では種々の大きさの血小板が混在している。ほとんどのBSS患者巨核球の数は正常

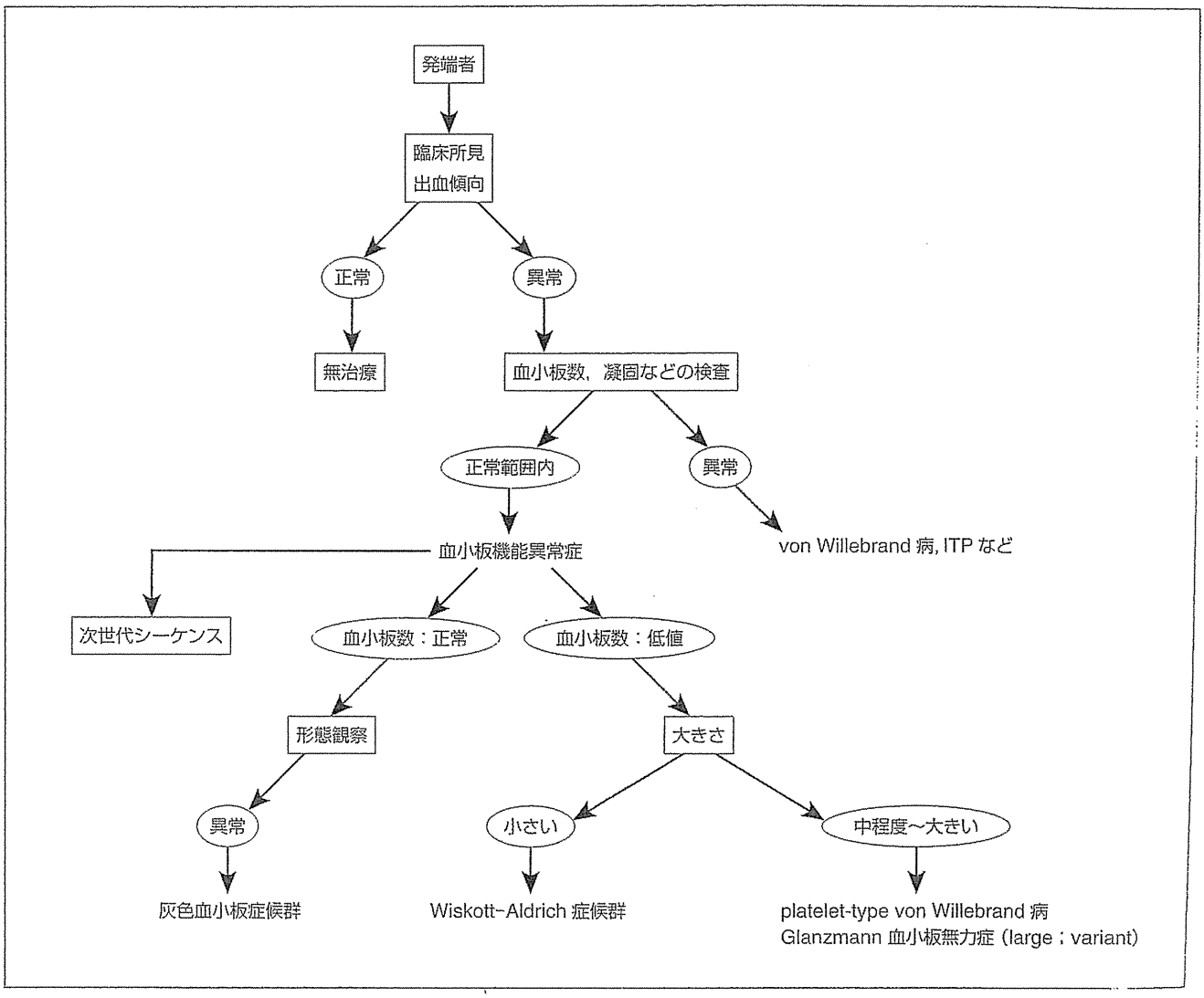

図5　先天性血小板機能異常の診断フローチャートの提案
Dr. Paolo Gresele の講演内容を簡略化した著者のメモをもとに作成
ITP：特発性血小板減少性紫斑病

であり，血小板数は 20,000～30,000/μL と著明な減少例から，わずかに減少している例まで様々である。これらの報告から，BSS 患者に認められる巨大血小板は，血小板産生過程の最終段階の制御機構に問題が生じていると考えられる。BSS 患者血小板はリストセチン惹起血小板凝集低下が認められる。他の惹起剤使用においては正常な血小板凝集能を示す[8]。

また，この GPⅠbα の遺伝子変異により血小板減少と巨大血小板を示す platelet-type von Willbrand（フォン・ヴィルブランド）病（PT-VWD）が報告されているが，遺伝子変異により VWF との結合能が増加することで血小板が消化された結果として血小板減少を呈している[9]。PT-VWD の原因となる遺伝子変異の場所は集中している。PT-VWD 患者の血小板は，低濃度リストセチンにより血小板凝集が惹起される。これらの因子は膜受容体であり，リガンドとの結合を介して血小板機能発現に重要な役割を有するとともに，血小板産生の過程においても非常に重要な役割を有している。

非筋ミオシン重鎖ⅡA をコードする MYH9 の遺伝子変異は，MYH 異常症として包括されている May-Hegglin（メイ-ヘグリン）異常症，Sebastian（セバスチャン）血小板症候群，Fechtner（フェクトナー）症候群，Epstein（エプスタイン）症候群の原因となる。いずれも血小板減少と巨大血小板が認められる。白血球封入体は，May-Hegglin 異常症，Sebastian 血小板症候群，Fechtner 症候群で認められ，Alport（アルポート）症状は，

Fechtner 症候群，Epstein 症候群で認められる。しかし，MYH9 の遺伝子変異はいずれの場所のものでも巨核球分化に影響はないと考えられている。また，その遺伝子変異はいずれの場所のものでも proplatelet 形成に関与していると考えられている[10]。

GATA1 は，造血幹細胞から赤芽球系，巨核球系の成熟分化に重要であると報告されている転写因子である。その遺伝子変異により血小板減少，巨大血小板，赤血球系の形態異常を認める。しかし，GATA1 の遺伝子変異や GATA1 欠損の細胞において，十分量ではないが血小板の産生が認められる。これは，GATA2 が GATA1 の働きを代替するためと報告されている。neurobeachin-like 2 が顆粒形成異常で血小板減少を示す灰色血小板(gray platelet)症候群の原因遺伝子変異を有すると最近報告された[11)~14)]。灰色血小板症候群患者の血小板は巨大なものが混在している。顆粒球においても，正常な顆粒と灰色に観察できる形成異常の顆粒が混在して認められる。

β_1-tubulin は成熟巨核球，血小板に特異的に発現し，血小板の細胞骨格形成や血小板機能発現に非常に重要な働きを有している。その β_1-tubulin の遺伝子変異により血小板減少と巨大血小板が認められる。細胞膜の安定性保持に重要な役割を有する ANKRD26 の遺伝子変異により血小板減少をきたす。巨核球はやや減少する。c-MPL (myeloproliferative protein) は血小板分化に重要な因子であるトロンボポエチンの受容体である。この c-MPL の遺伝子変異により，巨核球の著減と血小板減少を示す[15]。

Wiskott-Aldrich(ウィスコット-アルドリッチ)症候群(WAS)蛋白の遺伝子変異は，WAS の原因となる。血小板減少，血小板サイズは小さく，平均血小板容積(mean platelet volume：MPV)は低値を示す。巨核球は正常か増加を示す。WASP 遺伝子変異により血小板減少のみを呈する X 連鎖血小板減少症(X-linked thrombocytopenia：XLT)もある[16]。GPⅡb/Ⅲa の遺伝子変異による血小板無力症は，血小板機能異常を呈する。血小板数や形態には異常を認めないが，血小板凝集能検査ではリストセチンを除く惹起剤での血小板凝集欠如が認められる。血小板無力症には GPⅡb/Ⅲa の質的・量的異常が存在する。

おわりに

本稿では，止血機構における血小板の役割，特に血小板の量的・質的異常による出血傾向に関しては引用文献を多く記載して概説した。本稿が出血傾向患者に向きあった際の一助になれば幸いである。

【松原 由美子・村田 満】

参考文献

1) Versteeg HH et al：New fundamentals in hemostasis. Physiol Rev 93：327-358, 2013
2) Stalker TJ et al：Platelet signaling. Handb Exp Pharmacol 210：59-85, 2012
3) 松原由美子ほか：血栓形成の分子機構．血栓と循環 13：12-16, 2005
4) Mezzano D et al：The level of laboratory testing required for diagnosis or exclusion of a platelet function disorder using platelet aggregation and secretion assays. Semin Thromb Hemost 35：242-254, 2009
5) Malara A et al：Blood platelet production and morphology. Thromb Res 129：241-244, 2012
6) Barbour T et al：Thrombotic microangiopathy and associated renal disorders. Nephrol Dial Transplant 27：2673-2685, 2012
7) 藤村欣吾ほか：成人特発性血小板減少性紫斑病治療の参照ガイド 2012 年版．臨床血液 53：433-442，2012
8) Lanza F：Bernard-Soulier syndrome (hemorrhagiparous thrombocytic dystrophy). Orphanet J Rare Dis 16：46, 2006
9) Othman M：Platelet-type von Willebrand disease：a rare, often misdiagnosed and underdiagnosed bleeding disorder. Semin Thromb Hemost 37：464-469, 2011
10) Balduini CL et al：Recent advances in the understanding and management of MYH9-related inherited thrombocytopenias. Br J Haematol 154：161-174, 2011
11) Gunay-Aygun M et al：Gray platelet syndrome：natural history of a large patient cohort and locus assignment to chromosome 3p. Blood 116：4990-5001, 2010
12) Kahr WH et al：Mutations in NBEAL2, encoding a BEACH protein, cause gray platelet syndrome. Nat Genet 43：738-740, 2011
13) Gunay-Aygun M et al：NBEAL2 is mutated in gray platelet syndrome and is required for biogenesis of platelet α-granules. Nat Genet 43：732-734, 2011
14) Albers CA et al：Exome sequencing identifies NBEAL2 as the causative gene for gray platelet syndrome. Nat Genet 43：735-737, 2011
15) Geddis AE：Congenital amegakaryocytic thrombocytopenia. Pediatr Blood Cancer 57：199-203, 2011
16) Notarangelo LD：Wiskott-Aldrich syndrome. Curr Opin Hematol 15：30-36, 2008

The Journal of Immunology

Innate Response to Human Cancer Cells with or without IL-2 Receptor Common γ-Chain Function in NOD Background Mice Lacking Adaptive Immunity

Chiyoko Nishime, Kenji Kawai, Takehiro Yamamoto, Ikumi Katano, Makoto Monnai, Nobuhito Goda, Tomoko Mizushima, Hiroshi Suemizu, Masato Nakamura, Mitsuru Murata, Makoto Suematsu and Masatoshi Wakui

J Immunol 2015; 195:1883-1890; Prepublished online 13 July 2015;
doi: 10.4049/jimmunol.1402103
http://www.jimmunol.org/content/195/4/1883

The Journal of Immunology is published twice each month by
The American Association of Immunologists, Inc.,
9650 Rockville Pike, Bethesda, MD 20814-3994.

Print ISSN: 0022-1767 Online ISSN: 1550-6606.

Innate Response to Human Cancer Cells with or without IL-2 Receptor Common γ-Chain Function in NOD Background Mice Lacking Adaptive Immunity

Chiyoko Nishime,*,† Kenji Kawai,† Takehiro Yamamoto,* Ikumi Katano,† Makoto Monnai,† Nobuhito Goda,‡ Tomoko Mizushima,† Hiroshi Suemizu,† Masato Nakamura,§ Mitsuru Murata,¶ Makoto Suematsu,*,‖ and Masatoshi Wakui¶

Immunodeficient hosts exhibit high acceptance of xenogeneic or neoplastic cells mainly due to lack of adaptive immunity, although it still remains to be elucidated how innate response affects the engraftment. IL-2R common γ-chain (IL-2Rγc) signaling is required for development of NK cells and a subset of dendritic cells producing IFN-γ. To better understand innate response in the absence of adaptive immunity, we examined amounts of metastatic foci in the livers after intrasplenic transfer of human colon cancer HCT116 cells into NOD/SCID versus NOD/SCID/IL-2Rγc^{null} (NOG) hosts. The intravital microscopic imaging of livers in the hosts depleted of NK cells and/or macrophages revealed that IL-2Rγc function critically contributes to elimination of cancer cells without the need for NK cells and macrophages. In the absence of IL-2Rγc, macrophages play a role in the defense against tumors despite the NOD *Sirpa* allele, which allows human CD47 to bind to the encoded signal regulatory protein α to inhibit macrophage phagocytosis of human cells. Analogous experiments using human pancreas cancer MIA PaCa-2 cells provided findings roughly similar to those from the experiments using HCT116 cells except for lack of suppression of metastases by macrophages in NOG hosts. Administration of mouse IFN-γ to NOG hosts appeared to partially compensate lack of IL-2Rγc–dependent elimination of transferred HCT116 cells. These results provide insights into the nature of innate response in the absence of adaptive immunity, aiding in developing tumor xenograft models in experimental oncology. ***The Journal of Immunology*, 2015, 195: 1883–1890.**

A number of immunodeficient mouse strains have been widely used as hosts in experimental transplantation models (1). High acceptance of xenogeneic or neoplastic cells is exhibited mainly due to lack of adaptive immunity resulting from failure in development of thymus-dependent T cells in strains bearing *nu* locus or in development of both T cells and B cells in strains bearing *scid* locus or disrupted *Rag* gene. Additionally, genetic introduction of impaired innate immunity onto strains lacking adaptive immunity also has been applied to the development of hosts more highly accepting xenogeneic or neoplastic cells, represented by the introduction of null gene of IL-2R common γ-chain (IL-2Rγc) or NOD background onto the strains having *scid* locus or disrupted *Rag* gene (2). IL-2Rγc signaling is required for development of NK cells and a subset of dendritic cells (DCs) producing IFN-γ represented by the CD11c$^+$B220$^+$ CD122$^+$ phenotype (3, 4). The allele of *Sirpa* gene in the NOD background mice allows human CD47 to bind to the encoded signal regulatory protein α (sirpa) to inhibit macrophage phagocytosis of human cells (5, 6). The details of how such alteration in innate immunity contributes to the engraftment are of considerable interest but still remain to be elucidated.

To better understand innate response in the absence of adaptive immunity, we examined amounts of metastatic foci in the livers after intrasplenic transfer of human colon cancer HCT116 cells to NOD/SCID versus NOD/SCID/IL-2Rγc^{null} (NOG) hosts using intravital microscopic imaging combined with in vivo depletion of NK cells and macrophages. The results demonstrated a line of evidence for contribution of innate effectors other than NK cells and macrophages in the presence of IL-2Rγc versus of macrophages in the absence of IL-2Rγc to elimination of human cancer cells in the NOD background hosts lacking adaptive immunity.

Materials and Methods

Cells

A human colon cancer cell line HCT116 and a human pancreas cancer cell line MIA PaCa-2 were obtained from the American Type Culture Collection (Manassas, VA). HCT116 cells were maintained in McCoy's 5A (Sigma-Aldrich, St. Louis, MO) containing antibiotics and 10% FBS (HyClone, Logan, UT). MIA PaCa-2 cells were maintained in DMEM (Sigma-Aldrich) containing antibiotics, 10% FBS, and 2.5% horse serum. HCT116 and MIA PaCa-2 cells were incubated in a humidified (37°C, 5% CO_2) incubator and passaged on reaching 80% confluence.

*Department of Biochemistry, School of Medicine, Keio University, Shinjuku-ku, Tokyo 160-8582, Japan; †Central Institute for Experimental Animals, Kawasaki-ku, Kawasaki, Kanagawa 210-0821, Japan; ‡Department of Life Science and Medical Bio-Science, School of Advanced Science and Engineering, Waseda University, Shinjuku-ku, Tokyo 162-8480, Japan; §Department of Pathology, Tokai University School of Medicine, Shimokasuya, Isehara, Kanagawa 259-1193, Japan; ¶Department of Laboratory Medicine, School of Medicine, Keio University, Shinjuku-ku, Tokyo 160-8582, Japan; and ‖Japan Science and Technology Agency, Exploratory Research for Advanced Technology Suematsu Gas Biology Project, Shinjuku-ku, Tokyo 160-8582, Japan

Received for publication August 18, 2014. Accepted for publication June 13, 2015.

This work was supported by the Keio University Global Center of Excellence Program, the Leading Project for Biosimulation, and Japan Society for the Promotion of Science Grant-in-Aid for Scientific Research (C) 25430139, all of which were funded by the Ministry of Education, Culture, Sport, Science and Technology, Japan.

Address correspondence and reprint requests to Dr. Masatoshi Wakui, Department of Laboratory Medicine, School of Medicine, Keio University, 35 Shinanomachi, Shinjuku-ku, Tokyo 160-8582, Japan. E-mail address: wakuism@a6.keio.jp

The online version of this article contains supplemental material.

Abbreviations used in this article: Cl_2MDP-liposome, dichloromethylene diphosphonate–containing liposome; DC, dendritic cell; IL-2Rγc, IL-2R common γ-chain; MDSC, myeloid-derived suppressor cell; NOG, NOD/SCID/IL-2Rγc^{null}; sirpa, signal regulatory protein α.

www.jimmunol.org/cgi/doi/10.4049/jimmunol.1402103

Preparation of the pcDNA3.1/Venus vector

Venus has been developed by mutagenesis engineering as an improved version of yellow fluorescent protein, which is derived from GFP variants (7). Venus is fully and stably fluorescent due to its resistance to pH and chloride ion. The original vector containing the Venus gene sequence was gifted from Dr. Atsushi Miyawaki (Brain Science Institute, RIKEN, Saitama, Japan). The Venus gene fragments were amplified by PCR and then purified through electrophoresis. These PCR products were inserted in the pcDNA3.1/myc-His(−)A vector (Invitrogen, Carlsbad, CA) at XbaI and KpnI sites with a DNA ligation kit (Takara Bio, Shiga, Japan), followed by cloning using XL2-Blue MRF′ ultracompetent cells (Strategene, La Jolla, CA). It was confirmed by sequencing that the cloned pcDNA3.1/Venus vector plasmids keep the Venus gene sequence without any mutational alteration.

Venus gene transduction of human colon cancer cells

The Venus gene transduction of HCT116 cells was carried out using Lipofectamine 2000 (Invitrogen) as recommended by the manufacturer. The cells were treated with G418 (Invitrogen) at final concentration of 1.0 mg/ml for selection of positive clones 2 d after transduction and then cultured for a week. The Venus expression on selected clones was evaluated by flow cytometric analysis using Epics XL-MCL (Beckman Coulter, Brea, CA).

Liver metastasis assay

The in vivo experiments were performed in accordance with institutional guidelines and approved by the Animal Experimentation Committee of the Keio University and the Central Institute for Experimental Animals. We bred NOD/Shi-*scid* (NOD/SCID) and NOG mice and used them at the age of 9–11 wk. Liver metastases were induced by intrasplenic transfer of HCT116 cells, followed by splenectomy (8). In the case of transfer of 1×10^6 cells, the mice were subjected to the intravital microscopic bioimaging within 30 min or 1–2 wk later as described below. After the intravital microscopic studies, the mice were sacrificed and liver metastases were enumerated immediately.

Intravital microscopic imaging

The intravital observation of livers after intrasplenic transfer of fluorescently visualized HCT116 cells expressing Venus was performed with an in vivo video microscopic method as reported previously (9, 10). For each experimental group, four to five mice were examined. The mouse was placed on an inverted microscope platform, the disk scan unit system (IX81-DSU; Olympus, Tokyo, Japan), after abdominal section. For each mouse, microscopic observations on six to nine hepatic lobules were recorded using the electron multiplying CCD camera (Cascade II; Nippon Roper, Tokyo, Japan) and the MetaMorph software (MDS, Toronto, ON, Canada).

Evaluation of metastatic foci of HCT116 cells in the bioimaging data

Based on the obtained bioimaging data and histological findings, terminal portal venules and centrilobular venules were identified in examined hepatic lobules. The measurement of distances between a terminal portal venule and the closest centrilobular venule was performed using the Scion image software (Scion, Frederick, MD), indicating that the average distance was 320.4 ± 66.7 μm. Considering this value, each C point was used as the center to draw a circle at the radius of 320 μm, which reflected a putative hepatic lobule. Each circle was divided into three zones, that is, the periportal zone, the middle zone, and the pericentral zone. The area of each metastatic focus of fluorescently visualized HCT116 cells expressing Venus was measured and then the percentages of tumor lesion in the periportal, middle, and pericentral zones were calculated.

Evaluation of metastatic foci of MIA PaCa-2 cells using immunohistochemistry

Sections (3-μm-thick) were cut from paraffin-embedded tissue blocks. Immunostaining of the section with a mouse anti-HLA class I (A, B, and C) mAb (clone EMR8-5; Hokudo, Sapporo, Japan) was performed on the Bond-Max automated IHC platform (Leica Biosystems, Mount Waverley, Australia). The photographic images of the immunostained sections were prepared by Axio Imager.M1 (Carl Zeiss, Thornwood, NY) and then converted to the grayscale images using Photoshop CC 2014 (Adobe Systems, San Jose, CA). The measurement of metastatic foci of MIA PaCa-2 cells visualized immunohistochemically with HLA class I expression was carried out using the software ImageJ version 1.48 (http://imagej.nih.gov/ij/).

Depletion of NK cells and macrophages

To deplete only NK cells, NOD/SCID mice were i.p. given 400 μl PBS containing 20 μl anti-asialo GM1 antiserum (Wako, Osaka, Japan) on days −3, −2, and −1, followed by intrasplenic transfer of human cancer cells on day 0 (3). To deplete both NK cells and macrophages, NOD/SCID mice were i.p. given 400 μl PBS containing 20 μl anti-asialo GM1 antiserum on days −3, −2, and −1, followed by treatment for macrophage depletion on day −2 as describe below and then by intrasplenic transfer of human cancer cells on day 0. To deplete macrophages, dichloromethylene diphosphonate–containing liposomes (Cl_2MDP-liposomes) were prepared as described previously (11). NOD/SCID and NOG mice were i.v. given Cl_2MDP-liposomes suspended in 100 μl PBS on day −2, followed by intrasplenic transfer of human cancer cells on day 0.

IFN-γ treatment

NOG mice were i.p. given mouse rIFN-γ at a dose of 1×10^5 units 1 d before transfer of HCT116 cells as reported previously (12).

Isolation and transfer of the DC subset

Spleens from NOD/SCID mouse were minced and digested with 0.1% collagenase (Roche Diagnostics, Laval, QC, Canada) and DNase (1 mg/ml; Wako Pure Chemical Industries, Osaka, Japan) at 37°C for 30 min. After washing with 2% FCS in PBS, cells were stained with biotinylated mouse B220 Ab (BioLegend, San Diego, CA) and incubated with anti-biotin magnetic beads (Miltenyi Biotec, Sunnyvale, CA) to isolate the DC subpopulation. $B220^+$ and $B220^-$ fractions were separated on a MACS column (Miltenyi Biotec) and the enriched $B220^+$ fractions were stained with PE-labeled CD11c Ab (BioLegend). The $B220^+CD11c^+$ cells were sorted using the BD FACSAria II cell sorter (BD Biosciences, San Jose, CA). The purity level of $B220^+CD11c^+$ was 96.1%. RBCs of the $B220^-$ cell fraction were lysed in Pharm Lyse buffer (BD Biosciences) and washed with 2% FCS in PBS. The purified $B220^+CD11c^+$ cells and $B220^-$ cells were resuspended in RPMI 1640 (Corning, Tewksbury, MA), and 1×10^5 cells were transferred i.v. into NOG mice 1 d before transfer of HCT116 cells.

Immunohistochemistry for hepatic macrophages

Sections (3 μm thick) were cut from paraffin-embedded tissue blocks. To reveal distribution of hepatic macrophages, immunostaining of liver tissues was carried out with a rat anti-mouse F4/80 mAb (Bio-Rad/AbD Serotec, Kidlington, U.K.) and a rabbit anti-mouse Ym-1 polyclonal Ab (Stemcell Technologies, Carlsbad, CA) and performed with Bond-Max automated immunostainer (Leica Biosystems). Sections were counterstained with hematoxylin.

Statistical analysis

The statistical significance of data among different experimental groups was determined by Student *t* test or one-way ANOVA, and a p value < 0.05 was considered significant.

Results

Intravital microscopic imaging reveals the early events in the liver metastasis model with HCT116 cells expressing Venus

As with parental HCT116 cells, HCT116 cells expressing Venus (termed HCT116/Venus cells) robustly metastasized in NOG but not in NOD/SCID hosts. Fig. 1 shows the representative results. One week after the transfer of 1×10^6 HCT116/Venus cells, amounts of metastatic foci were microscopically evident preferentially in periportal regions of the livers in NOG but not in NOD/SCID hosts; all of five NOG mice versus none of five NOD/SCID mice exhibited microscopic metastases. At that time, macroscopic metastases were not observed in any of the five NOG or NOD/SCID mice. By 2 wk after the transfer, the hepatic metastases were developed macroscopically in NOG but not in NOD/SCID hosts; all of five NOG mice versus none of five NOD/SCID mice exhibited macroscopic metastases. At that time, microscopic metastases were observed in just one of the five NOD/SCID mice, looking tiny and morphologically fragile. Even 3 wk after the transfer, only two of five NOD/SCID mice exhibited macroscopic metastases, which were observed as a small number of tiny nodules in the livers.

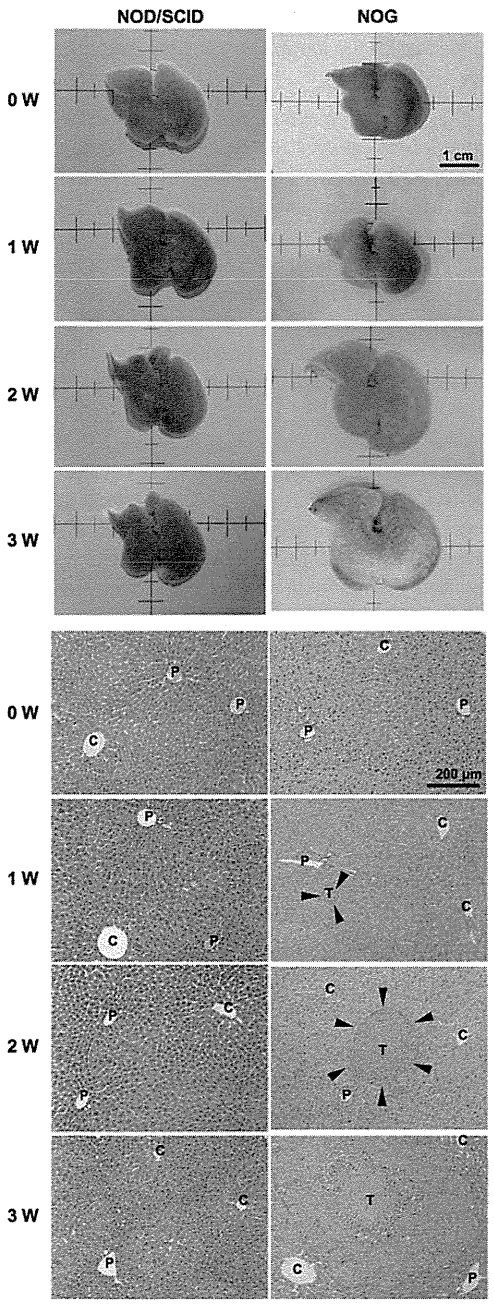

FIGURE 1. Robust formation of metastatic foci of human colon cancer HCT116 cells occurs in the liver of NOG hosts. Macroscopic and microscopic (H&E staining) findings of the livers in NOD/SCID versus NOG hosts at indicated time points after transfer of 1×10^6 HCT116/Venus cells are shown. C, centrilobular venules; P, terminal portal venules; T, tumor.

To assess differences in events occurring immediately after intrasplenic transfer of human cancer cells between the two strains, the intravital microscopic imaging was applied. Transfer of 1×10^6 HCT116/Venus cells to each host was suitable for the bioimaging analysis. Within 30 min after the transfer, arrest of HCT116/Venus cells inside sinusoids of periportal regions of hepatic lobules was observed similarly in both strains (Fig. 2A). The distribution of arrest of HCT116/Venus seemed to overlap with preferential location of hepatic macrophages. It was of considerable interest whether macrophages participated in trapping of human cancer cells transferred intrasplenically. The in vivo macrophage-depletion experiments using Cl_2MDP-liposomes in NOD/SCID and NOG hosts revealed that the cancer cell arrest inside hepatic sinusoids occurred independently of macrophages (Fig. 2B, 2C).

Hepatic micrometastatic foci are formed in NOG but not in NOD/SCID mice and distributed similarly to the initial cancer cell arrest

One week after the transfer, amounts of metastatic foci were microscopically evident preferentially in periportal regions of the lobules in NOG mice but were not detected in any hepatic area of NOD/SCID mice (Figs. 1, 3A). The distribution of micrometastases was similar to that of the arrest of HCT116/Venus cells within 30 min after the transfer, suggesting that the micrometastatic foci originated from cancer cells arrested initially after the intrasplenic transfer.

Macrophages play a role in the defense against hepatic metastases in NOG mice

Macrophages have potentials not only to kill tumor cells but also to promote tumor progression via several mechanisms, such as proangiogenic and immunosuppressive actions, under some conditions (13). To assess how host macrophages influence the tumor formation, we compared metastatic foci of HCT116/Venus cells in NOG hosts in in vivo–depleted and nondepleted of macrophages. As shown in Fig. 3B, macrophages were found to suppress hepatic metastases in NOG mice.

Rejection of transferred HCT116 cells occurring in NOD/SCID but not in NOG mice does not require NK cells or macrophages

Although it is thought that lack of NK cells is one of the most critical features with respect to the immunodeficiency of NOG mice, loss not only of NK cell–dependent but also of NK cell–independent mechanisms contribute to superior reconstitution of human hematopoietic tissues (3, 4). To assess the dependences of antitumor effects on NK cells in NOD/SCID hosts, in vivo depletion experiments were carried out using anti-asialo GM1 Ab treatment, analogous to the previous study (3). NK cell depletion failed to initiate hepatic metastases of HCT116 cells in any NOD/SCID hosts, revealing that the antitumor effects occurring with requiring IL-2Rγc were independent of NK cells (Fig. 4). Considering the suppressive effects of macrophages on hepatic metastases that were observed in NOG hosts as described above, metastatic foci in the livers were compared between NOD/SCID hosts depleted versus not depleted of macrophages. With or without in vivo NK cell depletion, macrophage depletion also failed to initiate hepatic metastases of HCT116 cells in contrast to the case of NOG hosts (Fig. 4). These results provided evidence that IL-2Rγc–dependent tumor elimination in NOD/SCID hosts does not require NK cells or macrophages.

Analogous experiments using MIA PaCa-2 cells provide findings roughly similar to those from experiments using HCT116 cells except for lack of suppression of metastases by macrophages in NOG hosts

To examine whether antitumor effects observed are limited to HCT116 cells, analogous experiments using human pancreas cancer MIA PaCa-2 cells were carried out (Fig. 5). Transferred MIA PaCa-2 cells formed a negligible amount of metastatic foci in the livers of NOD/SCID hosts whereas robust metastases occurred in the livers of NOG hosts. Consistent with the observations in the setting of HCT116 cells, depletion of NK cells and/or macrophages did not significantly affect MIA PaCa-2 metastases in NOD/SCID hosts. Alternatively, unlike the HCT116 metastases, the MIA PaCa-2 metastases were not affected by depletion of macrophages in NOG hosts.

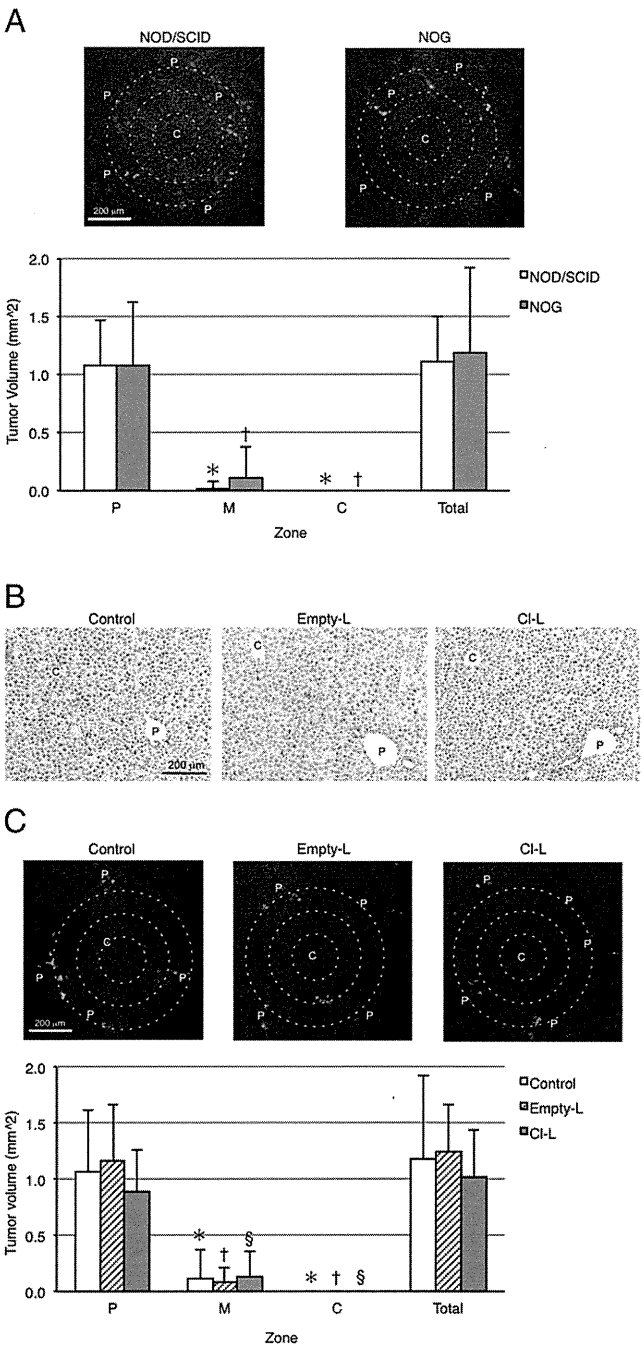

FIGURE 2. Arrest of HCT116 cells occurs inside sinusoids of periportal regions of hepatic lobules immediately after intrasplenic transfer to NOD/SCID and NOG hosts. (**A**) Amounts and distributions of metastatic foci were intravitally evaluated within 30 min after the intrasplenic transfer to NOD/SCID and NOG mice by detecting the fluorescence of HCT116/Venus cells. (**B**) Representative results of immunohistochemical staining with F4/80 for detection of hepatic macrophages in NOG mice undergoing indicated treatments are shown. (**C**) Amounts and distributions of metastatic foci were intravitally evaluated within 30 min after the intrasplenic transfer to hosts undergoing indicted treatments. Representative results from NOG hosts are shown. Columns show mean; bars indicate SD. Outer white broken circles demarcate the periportal (P) zone, middle white broken circles demarcate the middle (M) zone, and inner white broken circles demarcate the pericentral (C) zone. (A) $^{*}p < 0.05$, statistically significant difference when compared with metastatic foci located at different zones of NOD/SCID hosts; $^{\dagger}p < 0.05$, statistically significant difference when compared with metastatic foci located at different zones of NOG hosts. (C) $^{*}p < 0.05$, statistically significant difference when compared with metastatic foci located at different zones in NOG hosts treated with saline; $^{\dagger}p < 0.05$, statistically significant difference when compared with metastatic foci located at different zones in NOG hosts treated with empty-liposomes; $^{\S}p < 0.05$, statistically significant difference when compared with metastatic foci located at different zones in NOG hosts treated with Cl_2MDP-liposomes. C, centrilobular venules; Cl-L, treatment with Cl_2MDP-liposomes; Control, treatment with saline; Empty-L, treatment with empty-liposomes; P, terminal portal venules.

Distribution of F4/80$^+$ cells and Ym1$^+$ cells in MIA PaCa-2 metastatic foci differs from that in HCT116 metastatic foci in NOG hosts

To assess the potential mechanisms by which macrophages play a role in the defense against metastases in NOG but not in NOD/SCID hosts, M1/M2 macrophage polarization in the metastatic foci was analyzed by immunohistochemistry (Fig. 6). The staining of liver sections with representative markers such as inducible NO synthase, CD40, CD86, and MHC class II was inconvenient to use for specific detection of M1 macrophages in the livers because they were expressed not only by macrophages but also by non-hematopoietic cells as reported previously (14–19). The staining with a representative marker Ym1 was useful to detect M2 macrophages in the liver (15). In the present study, F4/80$^+$ cells without Ym1 positivity were regarded as M1 macrophages whereas cells exhibiting concordance of Ym1 positivity with F4/80 positivity were regarded as M2 macrophages.

There were no obvious differences in M1/M2 polarization between intact NOD/SCID versus NOG mice, whereas remarkable differences in distribution of F4/80$^+$ cells and Ym1$^+$ cells were observed between HCT116 metastatic foci versus MIA PaCa-2 metastatic foci. There were few Ym1-expressing cells in contrast to a discernible number of F4/80$^+$ cells in the HCT116 metastatic foci, roughly consistent with M1 macrophage polarization. Alternatively, there were a considerable number of Ym1-expressing cells not only with but also without F4/80 positivity in the MIA PaCa-2 metastatic foci, suggesting macrophages less polarized to M1 type than those in the HCT116 metastatic foci. The F4/80$^-$ cells expressing Ym1 were distinct from typical M2 macrophages. Some of such cells were characteristic of morphologically immature granulocytes and others were mononuclear.

Lack of IL-2Rγc–dependent elimination of HCT116 cells in NOG mice appears to be partially compensated by administration of mouse IFN-γ

The absence of a subset of DCs producing IFN-γ is also one of the important characteristics of the immunodeficiency due to lack of IL-2Rγc (3, 4). To examine whether the endogenous IFN-γ production contributes to the antitumor effects depending on IL-2Rγc, we attempted to determine the impacts of in vivo neutralization using anti–IFN-γ Abs on antitumor effects occurring in NOD/SCID hosts. However, it was hard to optimize experimental conditions in NOD/SCID mice for stable and reproducible results. Alternatively, we examined effects of mouse IFN-γ administration on metastases of HCT116 cells in NOG hosts depleted or not depleted of macrophages. As shown in Fig. 7, with or without depletion of macrophages, the treatment of NOG hosts with recombinant mouse IFN-γ resulted in a significant decrease in hepatic HCT116 tumor burden but did not achieve such full eradication of tumors as occurred in NOD/SCID hosts. Thus, lack of the IL-2Rγc–dependent elimination of HCT116 cells without requiring NK cells and macrophages appeared to be partially compensated by the mouse IFN-γ administration.

To collect evidence for contribution of the IFN-γ–producing DC subset to the defense against tumors, we examined whether

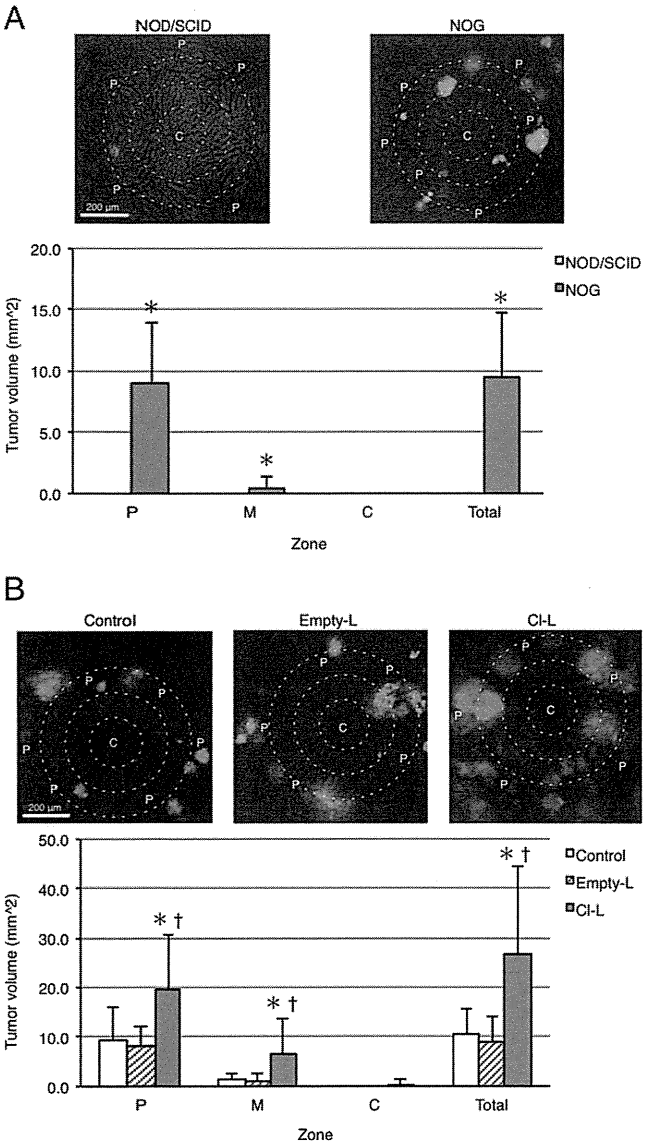

FIGURE 3. Hepatic metastatic foci appear in NOG but not in NOD/SCID hosts, distributing similarly to the initial cancer cell arrest. (**A**) Amounts and distributions of metastatic foci were intravitally evaluated 1 wk after the intrasplenic transfer to NOD/SCID and NOG mice by detecting the fluorescence of HCT116/Venus cells. (**B**) Amounts and distributions of metastatic foci were intravitally evaluated 2 wk after the intrasplenic transfer to NOG mice undergoing indicated treatments. Columns show mean; bars indicate SD. Outer white broken circles demarcate the periportal (P) zone, middle white broken circles demarcate the middle (M) zone, and inner white broken circles demarcate the pericentral (C) zone. (A) $*p < 0.05$, statistically significant difference between NOD/SCID versus NOG hosts. (B) $*p < 0.05$, statistically significant difference between NOG hosts treated with Cl_2MDP-liposomes versus saline; $^{\dagger}p < 0.05$, statistically significant difference between NOG hosts treated with Cl_2MDP-liposomes versus empty-liposomes. C, centrilobular venules; Cl-L, treatment with Cl_2MDP-liposomes; Control, treatment with saline; Empty-L, treatment with empty-liposomes; P, terminal portal venules.

transfer of the DC subset from NOD/SCID mice to NOG hosts can reduce HCT116 metastases. The $B220^+CD11c^+CD122^+$ phenotype reportedly represents the IFN-γ–producing DC subset, but it was difficult to stably sort high purity and a sufficient number of $B220^+CD11c^+CD122^+$ cells. Alternatively, $B220^+CD11c^+$ cells were sorted from the spleens from NOD/SCID mice to prepare the DC subset used for the transfer to NOG hosts. Consistent with the

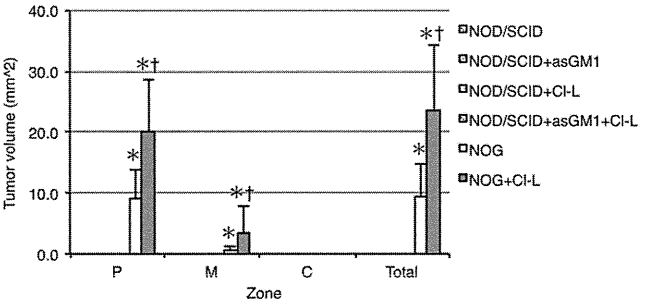

FIGURE 4. Antitumor effects occurring in NOD/SCID but not in NOG hosts do not require NK cells or macrophages. Amounts and distributions of metastatic foci were intravitally evaluated 1 wk after the intrasplenic transfer to NOD/SCID and NOG mice with or without in vivo depletion of NK cells and/or macrophages by detecting the fluorescence of HCT116/Venus cells. Columns show mean; bars indicate SD. asGM1, treatment with anti-asialo GM1 antiserum to deplete NK cells; Cl-L, treatment with Cl_2MDP-liposomes to deplete macrophages. $*p < 0.05$, statistically significant difference when compared with each group of NOD/SCID hosts; $^{\dagger}p < 0.05$, statistically significant difference between NOG hosts with versus without depletion of macrophages. C zone, pericentral zone; M zone, middle zone; P zone, periportal zone.

idea that the DC subset but not NK cells contributes to the innate response with IL-2Rγ function in the absence of adaptive immunity, the metastases tended to be reduced by the transfer of $B220^+CD11c^+$ cells from NOD/SCID mice to NOG hosts, although it did not achieve statistical significance ($p = 0.2710$) (Supplemental Fig. 1). An increased number of $B220^+CD11c^+$ cells or higher purity of the IFN-γ–producing DC subset transferred to NOG hosts might provide full findings to clarify whether the DC subset plays a leading role.

Discussion

The present study demonstrated a line of evidence for contribution of innate effectors other than NK cells and macrophages in the presence of IL-2Rγ_c versus macrophages in the absence of IL-2Rγ_c to eliminate human cancer cells. O'Sullivan et al. (14) reported on cancer immunoediting by the innate immune system in the absence of adaptive immunity. The report presented observations that NK cells contribute to regression of syngeneic tumors via their IFN-γ production to induce M1-type macrophages in the presence of IL-2Rγ_c. The apparent discrepancy from our findings revealing innate response without the need for NK cells and macrophages in the presence of IL-2Rγ_c seems to result from differences in immunoediting between the settings of syngeneic versus xenogeneic tumors. However, it is difficult to simply compare their findings and our findings because of the differences in experimental procedures. Notably, the in vivo depletion of NK cells was performed using anti-NK1.1 Ab in the study done by O'Sullivan et al. (14). This Ab might also deplete a subset of DCs expressing NK1.1, leading to loss of IFN-γ production by them as well as by NK cells (4). Note that observations from experiments with anti-NK1.1 Ab could not rule out the potential contribution of such DCs to innate response. Additionally, it was not ascertained in the previous study whether induced M1-type macrophages directly participate in the regression of syngeneic tumors, because functional experiments represented by in vivo depletion of macrophages that were performed in the current study were not carried out (14). At present, it appears that differences in immunoediting between the settings of syngeneic versus xenogeneic tumors still remain to be elucidated.

CD47 binds to sirpa to send a signal inhibiting phagocytosis by self-macrophages. Although mouse macrophages basically

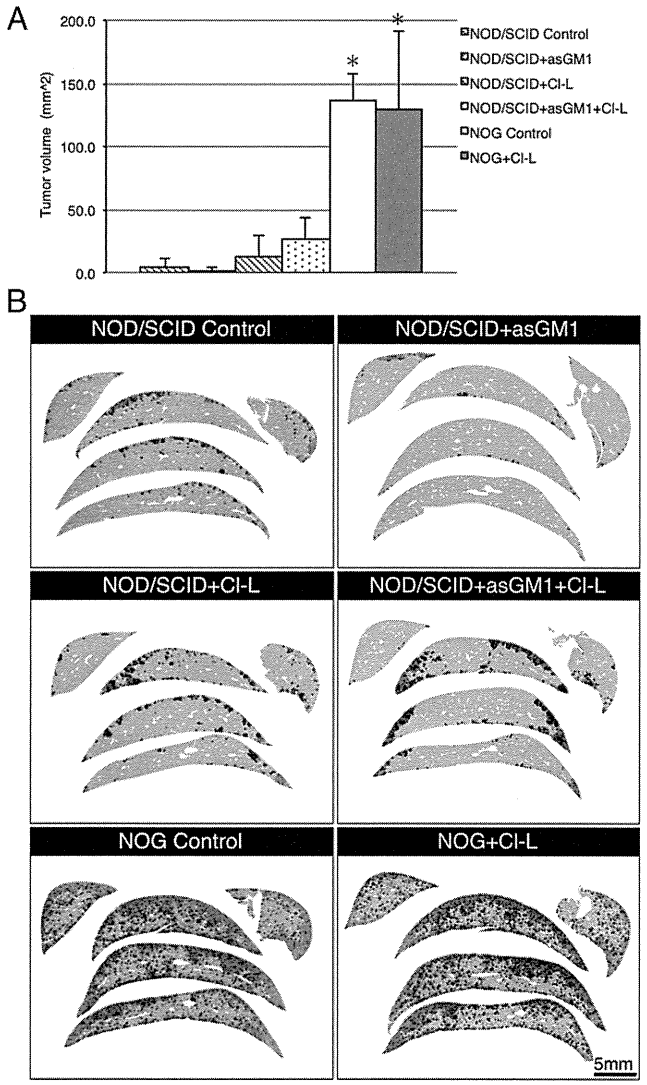

FIGURE 5. Analogous experiments using MIA PaCa-2 cells provide findings roughly similar to those from experiments using HCT116 cells except for lack of suppression of metastases by macrophages in NOG hosts. (**A**) Amounts of metastatic foci were immunohistochemically evaluated 2 wk after the intrasplenic transfer to NOD/SCID and NOG hosts undergoing indicated treatment by detecting HLA class I expression of MIA PaCa-2 cells. (**B**) Representative results of photographic imaging of immunostained sections are shown. Columns show mean; bars indicate SD. asGM1, treatment with anti-asialo GM1 antiserum to deplete NK cells; Cl-L, treatment with Cl_2MDP-liposomes to deplete macrophages; Control, treatment with saline. $*p < 0.05$, statistically significant difference when compared with each group of NOD/SCID hosts.

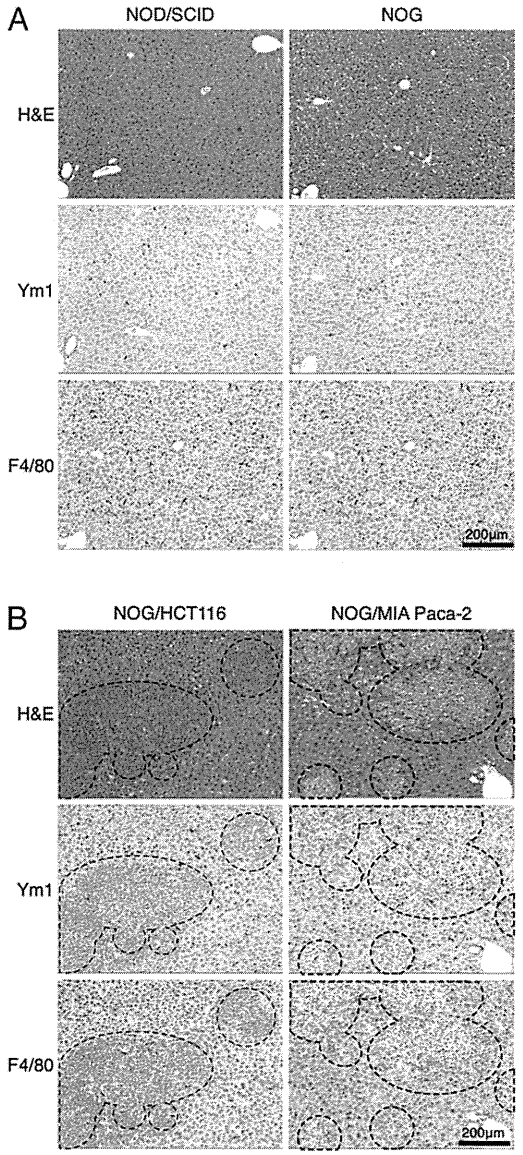

FIGURE 6. Distribution of $F4/80^+$ and $Ym1^+$ cells in MIA PaCa-2 metastatic foci differs from that in HCT116 metastatic foci in NOG hosts. (**A**) Representative results of histological examination of the livers in intact NOD/SCID versus NOG mice with indicated staining are shown. (**B**) Representative results of histological examination of HCT116 metastatic foci versus MIA PaCa-2 metastatic foci in the livers of NOG hosts with indicated staining are shown. Regions encircled by a broken line demarcate tumors.

eliminate xenogeneic cells due to inability of xenogeneic CD47 to bind to mouse sirpa, human CD47 can bind to sirpa encoded by the NOD-derived allele to avoid elimination of human cells by the NOD background macrophages (5, 6). Resembling hepatic metastases of HCT116 cells transferred to NOG hosts in the present study, reconstitution of human platelets and erythrocytes in the periphery was suppressed by host macrophages in contrast to that of leukocytes in the periphery and of all lineages of hematopoietic cells in the marrow in NOG hosts in previous studies (20, 21). Susceptibilities of human cells to elimination by NOG mouse macrophages may differ by cellular origin, differentiation, and neoplasticity.

As with NK cell development, IFN-γ production by DCs requires IL-15 signaling, which involves IL-2Rγc (22, 23). As expected, NOG mice lack IFN-γ produced by DCs (3). More recently, it has been revealed that a subset of DCs producing IFN-γ, which is represented by the $CD11c^+B220^+CD122^+$ phenotype, is absent from NOG mice (4). The decline in metastatic foci by mouse IFN-γ administration to NOG hosts appeared to reflect compensation for lack of the IL-2Rγc–dependent elimination of HCT116 cells via IFN-γ produced without requiring NK cells and macrophages. The IFN-γ–mediated effects to eliminate HCT116 cells should be exerted by IFN-γ–stimulated host cells owing to the absence of direct bioactivities of mouse IFN-γ on human cells (12). It is plausible that hematopoietic cells, such as granulocytes, and some nonhematopoietic cells are responsible for the antitumor effects induced by mouse IFN-γ administration to hosts lacking both macrophages and IL-2Rγc–dependent effectors. The possible mechanisms of antitumor effects triggered by IFN-γ include direct

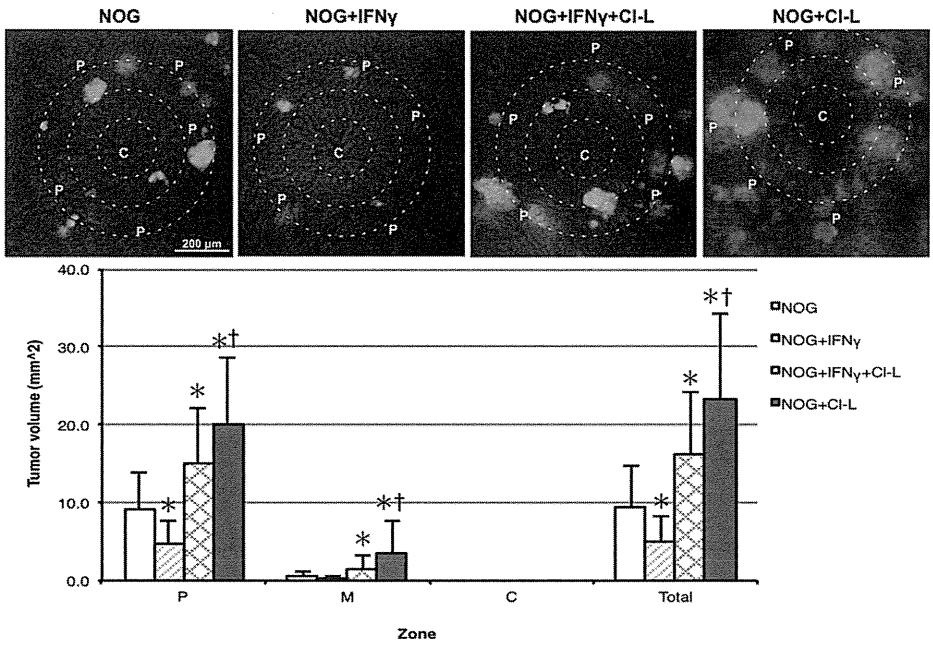

FIGURE 7. Lack of IL-2Rγc–dependent tumor elimination appears to be partially compensated by IFN-γ administration. Amounts and distributions of metastatic foci were intravitally evaluated 1 wk after the intrasplenic transfer to NOG mice undergoing indicated treatments by detecting the fluorescence of HCT116/Venus cells. Columns show mean; bars indicate SD. $*p < 0.05$, statistically significant difference when compared with NOG hosts without recombinant mouse IFN-γ treatment or macrophage depletion; $^{\dagger}p < 0.05$, statistically significant difference between recombinant mouse IFN-γ–treated versus nontreated NOG hosts depleted of macrophages. C, centrilobular venules; Cl-L, treatment with Cl_2MDP-liposomes to deplete macrophages; C zone, pericentral zone; IFN-γ, treatment with recombinant mouse IFN-γ; M zone, middle zone; P, terminal portal venules; P zone, periportal zone.

cellular attacks and indirect destruction via reactive oxygen species and NO produced by IFN-γ-stimulated cells (24). It is of considerable interest that the treatment of NOG hosts with IFN-γ did not achieve such full eradication of transferred HCT116 cells as occurred in NOD/SCID hosts even depleted of both NK cells and macrophages. This incompleteness suggests at least two possibilities. One is that a part of elimination of HCT116 cells may be mediated by IFN-γ–independent mechanisms in the presence of IL-2Rγ_c. Another is that innate cells producing IFN-γ dependently on IL-2Rγ_c function, which exist in NOD/SCID but not in NOG mice, may be also stimulated by IFN-γ to completely eradicate HCT116 cells.

IFN-γ has been reported to polarize macrophages toward M1 type (14, 15). However, there were no discernible differences in the M1/M2 macrophage ratio evaluated immunohistochemically between IFN-γ–treated versus nontreated NOG hosts undergoing HCT116 cell transfer (data not shown). Of note, the IFN-γ treatment reduced metastases in NOG hosts depleted of macrophages as well as those not depleted of macrophages. This suggests that skewing of M1/M2 macrophage ratio is less important to the mechanisms of effects of the IFN-γ treatment in NOG hosts. It is likely that M1 macrophage polarization is involved in innate response without, but not with, IL-2Rγ function.

The arrest of HCT116 cells inside sinusoids of periportal regions of hepatic lobules within 30 min after the transfer was not influenced by the presence of macrophages or IL-2Rγ_c–dependent effectors. The antitumor effects exerted with or without IL-2Rγ_c function appeared to require a priming phase after the transfer of HCT116 cells, suggesting that stimuli related to the transplantation procedures, such as debris of transferred cells, may trigger innate response to eliminate tumors (25).

The analogous experiments using MIA PaCa-2 cells also revealed that innate response to tumor cells does not require NK cells or macrophages in the presence of IL-2Rγ_c function, although evidence for suppression of metastases by macrophages in the absence of IL-2Rγ_c function was lacking, unlike the experiments using HCT116 cells. In intact livers of mice not undergoing transfer of tumor cells, M1/M2 macrophage polarization was roughly similar in NOD/SCID and NOG strains because of lacking obvious differences in the distribution of F4/80$^+$ cells and Ym1-expressing cells in the livers. Alternatively, given that the HCT116 metastases increased by macrophage depletion as well as the discernible predominance of F4/80$^+$ cells lacking Ym1 expression in the HCT116 metastatic foci, M1 macrophages likely contribute to the defense in NOG hosts.

A considerable number of Ym1-expressing cells in MIA PaCa-2 metastatic foci were not only localized out of distribution of F4/80$^+$ cells but were also morphologically distinct from macrophages. Some such cells resembled immature granulocytes. Ym1 has been reportedly expressed not only by macrophages but also by immature granulocytes, monocytes, and myeloid progenitor cells (26–28). Myeloid-derived suppressor cells (MDSCs), a heterogeneous population of myeloid cells, including granulocytic or monocytic characteristics, are recognized as a key player in escape from immune response and tumor progression. In our preliminary study, MDSCs defined by coexpression of Gr1 and CD11b, especially granulocytic MDSCs, which highly express Gr1, were increased in the peripheral blood of NOG mice after transfer of MIA PaCa-2 cells, compared with those after transfer of HCT116 cells and with those not undergoing any transfer (data not shown). A previous study has also shown expansion of MDSCs in NOD/SCID mice undergoing s.c. transplantation of MIA PaCa-2 cells (29). Taken together, it would be likely that non–macrophagic cells expressing Ym1 in the MIA PaCa-2 metastatic foci potentially represented MDSCs.

The lack of increase in MIA PaCa-2 metastases in NOG hosts depleted of macrophages would be explained by the idea that MIA PaCa-2 cells overcome or impair the macrophage response. Differences in the sensitivity to tumoricidal activities by macrophages between HCT116 versus MIA PaCa-2 cells still remain to be elucidated, although the predominance of Ym1-expressing cells over F4/40$^+$ cells in the metastatic foci suggests that MDSCs and/or M2 macrophages support MIA PaCa-2 tumor progression via inhibition of M1 macrophage polarization.

Collectively, comparison of observations between HCT116 metastases versus MIA PaCa-2 metastases may be a model to understand immunoediting via modulation of innate responses with or without IL-2Rγ function in tumor-bearing hosts that lack adaptive immunity. Considering the observations from the liver metastasis models using HCT116 cells and MIA PaCa-2 cells,